Stability and Folds

J. H. MADDOCKS

Communicated by H. WEINBERGER

Abstract

It is known that when one branch of a simple fold in a bifurcation diagram represents (linearly) stable solutions, the other branch represents unstable solutions. The theory developed here can predict instability of some branches close to folds, without knowledge of stability of the adjacent branch, provided that the underlying problem has a variational structure. First, one particular bifurcation diagram is identified as playing a special role, the relevant diagram being specified by the choice of functional plotted as ordinate. The results are then stated in terms of the shape of the solution branch in this distinguished bifurcation diagram. In many problems arising in elasticity the preferred bifurcation diagram is the load-displacement graph. The theory is particularly useful in applications where a solution branch has a succession of folds.

The theory is illustrated with applications to simple models of thermal self-ignition and of a chemical reactor, both of which systems are of Émden-Fowler type. An analysis concerning an elastic rod is also presented.

Contents

§ 1. Introduction

The basic role of a bifurcation diagram is to describe the solution set of some system of equations. However, it has long been realized that once a bifurcation diagram has been determined, either numerically or analytically, certain

conclusions concerning stability properties can be made with little or no additional analysis. The purpose of this work is to exploit the special structure of bifurcation problems that can be cast as variational principles to obtain particularly detailed predictions of stability properties.

The main result is the following:

Let $F(u, \lambda)$ be a real valued functional depending on a variable u and a bifurcation parameter λ, and suppose that F has branches of extremals (that is solutions of $F_u(\cdot, \lambda) = 0$) of the qualitative form depicted in Figure 1. Then, given certain regularity and nondegeneracy conditions, the lower branch in part (a), and the upper branch in part (b), represent extremals of F that are not local minima.

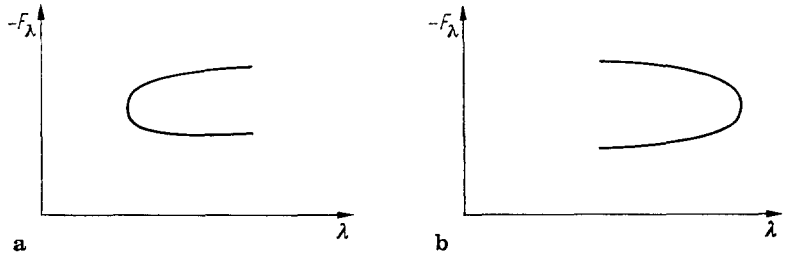

Fig. 1a and b. The two possible forms of a simple fold

To paraphrase, if the real valued functional $-F_\lambda \left(\text{i.e. } -\dfrac{\partial F}{\partial \lambda}\right)$ is chosen as the ordinate in a bifurcation diagram, then the lower branch of extremals in a fold opening to the right, and the upper branch in a fold opening to the left, cannot represent local minima of the functional F. The result is proven in § 2.

This theorem is obviously related to the "principle of exchange of stability" (see CRANDALL & RABINOWITZ 1973, SATTINGER 1972, or WEINBERGER 1978). The standard result predicts that if one branch of a simple fold represents local minima, then the other does not; the result is not sensitive to the functional chosen in the bifurcation diagram, or, indeed, to whether the ordinate is considered as a schematic representation of a function space. The result described above does not require the knowledge that one branch represents local minima, but it does require that the shape of the branch in one particular bifurcation diagram be known. The new result identifies the real-valued functional $-F_\lambda$ as determining upper and lower branches in such a way that "stability" predictions can be made.

The two theories are best contrasted when the branch of extremals has two successive folds, as is depicted in Figure 2.

Suppose that branch A is known to represent local minima. Then both theories predict that branch B cannot represent local minima. The standard theory can give no prediction concerning branch C, but the result presented above states that branch C in Figure 2(a) *does not* represent local minima. Moreover, with further genericity assumptions, the proof described in § 2 can be used to demonstrate that branch C in Figure 2(b) *does* represent local minima.

That the functional $-F_\lambda$ should play a distinguished role does, at first sight, appear strange. In fact the theory here presented can be rephrased in terms of the

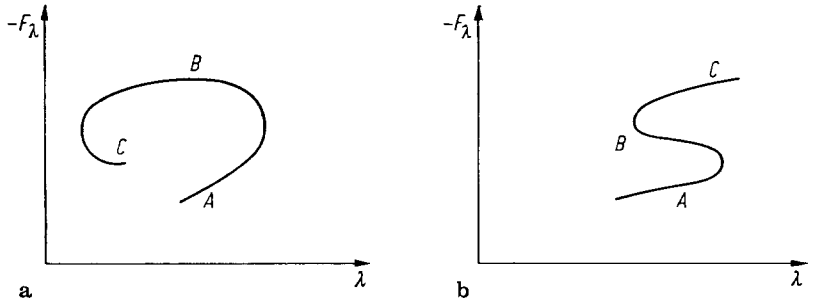

Fig. 2a and b. Two possible forms of two successive simple folds

functional $F(u, \lambda)$. The result is then the following: of the two branches associated with a fold, the one that realises the higher value of $F(u, \lambda)$ is unstable. This statement is intuitively obvious, at least in the finite-dimensional case, but both the analytical proof of the result, and its applications to the example of this paper are more straightforward when couched in terms of the functional $-F_\lambda$. The functional $F(u, \lambda)$ plays a more important role in the statement of the analogous results at bifurcation points. See MADDOCKS & JEPSON (1986).

In many physical problems the functional $F(u, \lambda)$ has the special form

$$F(u, \lambda) = G(u) - \lambda H(u),$$

in which the parameter λ appears linearly. The distinguished functional is then just $H(u)$. In particular, for many problems in elasticity that involve uniaxial loading, the resulting distinguished bifurcation diagram is the load-displacement graph.

Isoperimetric problems, in which λ plays the role of a Lagrange multiplier, are discussed in § 5; such problems have the form min $G(u)$, subject to $H(u) =$ const. The (H, λ) diagram can again be plotted, and the set of all extremals coincides with the extremals of min $(G - \lambda H)$. However, it will be shown that the folds critical to exchange of stability in the isoperimetric problem are the points of *horizontal* tangency to the solution branch, whereas points of *vertical* tangency are critical in the unconstrained problem.

Simple examples illustrating the theory are described in §§ 3, 4 and 6. It should be stressed that many of the results described in this work are already known in special cases and applications, to varying extents of generality and rigor. Prior works known to me are discussed in § 8.

§ 2. Proof of Result in Hilbert Space

Consider the following minimization problem:

$$\min_{u \in \mathscr{H}} F(u, \lambda). \tag{2.1}$$

Here $\mathscr{H}$ is a real Hilbert space, $F: \mathscr{H} \times R \to R$ is a functional with smooth dependence on both its arguments, and $\lambda \in R$ is a bifurcation parameter. A first-

order necessary condition for u to be a local minimum of F is that

$$F'(u, \lambda) = \mathbf{0}, \tag{2.2}$$

which can be regarded as an equation in $\mathscr{H}$ involving the Fréchet derivative of F with respect to u. This condition is essentially the Euler-Lagrange equation; we shall sometimes refer to (2.2) as the equilibrium equation.

It will be assumed that a branch of solutions to equation (2.2) is known; that is, there is a continuous curve of solutions $(u(s), \lambda(s)) \in \mathscr{H} \times R$, where s represents some parametrization. The choice of parametrization is deliberately left as general as is possible. It will be assumed that $\dot{u}(s) \left(= \frac{d}{ds} u\right) \in \mathscr{H}$ and $\dot{\lambda}(s) \in R$ exist, and that $\dot{u}^2 + \dot{\lambda}^2 \neq 0$.

A further necessary condition for u to be a local minimum of F (as opposed to merely being an extremal, or stationary point) is that the second variation of F at u be a nonnegative quadratic form. This second-order condition can be phrased as the requirement that the linear eigenvalue problem

$$F''(u, \lambda)\, \eta = \mu \eta, \quad \eta \in \mathscr{H}, \quad \mu \in R, \quad \langle \eta, \eta \rangle = 1, \tag{2.3}$$

has only non-negative eigenvalues. Here $F''(u, \lambda)(\cdot)$ is the second Fréchet derivative of F at the solution (u, λ); for each fixed u and λ it is a linear self-adjoint operator $\mathscr{H} \to \mathscr{H}$. Consequently all of its eigenvalues are real. Equation (2.3) can be regarded as the eigenvalue problem associated with Jacobi's accessory equation, *i.e.* the linearization of the Euler-Lagrange equation. The eigenvalues and eigenfunctions will be assumed to depend smoothly on the parameter s.

It is well known that equation (2.3) has the eigenvalue $\mu = 0$ whenever the solution (u, λ) is such that $\dot{\lambda} = 0$. To see this, differentiate the equilibrium equation along the solution branch to obtain

$$F''(u, \lambda)\, \dot{u} + \dot{\lambda} F'_\lambda(u, \lambda) = \mathbf{0}. \tag{2.4}$$

Here and subsequently the suscript λ connotes partial differentiation. Our focus of attention is the behavior of the critical eigenvalue close to points at which $\dot{\lambda} = 0$.

Definition. A point $(u(s_0), \lambda(s_0)) \in \mathscr{H} \times R$ on a smooth solution branch will be called a *fold* point if

$$\dot{\lambda}(s_0) = 0. \tag{2.5}$$

Recall that the parametrization was assumed to be chosen such that $\dot{u}^2 + \dot{\lambda}^2 \neq 0$. Accordingly, $\dot{u}(s_0)$ cannot be the null vector. A *simple* fold point satisfies the three additional conditions

$$\ddot{\lambda}(s_0) \neq 0, \tag{a}$$

$$\frac{d}{ds} F_\lambda \Big|_{s=s_0} \neq 0 \tag{b}$$

and (2.6)

zero is a simple eigenvalue of the operator $F''(u(s_0), \lambda(s_0))$. (c)

This definition of a simple fold is essentially standard, see, for example, DECKER & KELLER (1981). Close to any simple fold point the $-F_\lambda$ *vs.* λ bifurcation diagram must be of the form depicted in Figure 1, namely, there is a single smooth branch that lies either entirely to the left, or entirely to the right of the fold point. The $-F_\lambda$ *vs.* λ bifurcation diagram need not have this form close to a fold point at which any one of conditions (2.6) fails.

The main observation is that at a fold there is an elementary expression for $\dot{\mu}$, the derivative of the critical eigenvalue. Accordingly it is possible to characterize one particular branch as not representing local minima. To obtain the expression for $\dot{\mu}$, we write

$$\dot{u}(s) = \alpha(s)\,\eta(s) + \gamma(s), \quad \alpha(s) \in R, \tag{2.7}_1$$

where

$$\langle \eta, \eta \rangle = 1, \quad \langle \gamma, \eta \rangle = 0, \tag{2.7}_2$$

and η is understood to be the critical eigenfunction. The inner product of η with equation (2.4), then yields

$$\alpha\mu = -\dot{\lambda}\langle F'_\lambda, \eta \rangle,$$

which can be differentiated to provide the identity

$$\dot{\alpha}\mu + \alpha\dot{\mu} = -\ddot{\lambda}\langle F'_\lambda, \eta \rangle - \dot{\lambda}\frac{d}{ds}\langle F'_\lambda, \eta \rangle. \tag{2.8}$$

At a fold $\mu = 0$ and $\dot{\lambda} = 0$, which implies that at a simple fold $\gamma = 0$, or equivalently $\dot{u} = \alpha\eta$. Thus at a simple fold, (2.8) takes the form

$$\alpha^2(s)\,\dot{\mu}(s) = \ddot{\lambda}(s)\frac{d}{ds}\{-F_\lambda(u(s), \lambda(s))\}\Big|_{s=s_0}. \tag{2.9}$$

The first result can now be stated precisely.

Proposition 2.1. *Close to a simple fold opening to the* right, *the* lower *branch in a* $-F_\lambda$ vs. λ *bifurcation diagram* (cf. *Figure 1*(*a*)), *does not represent local minima. Similarly, close to a simple fold opening to the* left (cf. *Figure 1*(*b*)), *the* upper *branch does not represent local minima.*

Proof. At a simple fold neither $-\dot{F}_\lambda$ nor $\ddot{\lambda}$ vanishes. The sign of $-\dot{F}_\lambda$ can be chosen positive; this choice specifies that the parameter s is increasing as the fold is traversed from the lower to upper branch. The sign of $\ddot{\lambda}$ determines whether the fold opens to the right or to the left. The result follows from relation (2.9), because the critical eigenvalue μ is zero at the fold, and $\dot{\mu}$ is nonzero and its sign is determined. □

Remarks. (1) Analogous results for non-simple folds, are described at the end of this section.

(2) The choice of $-F_\lambda$ as ordinate is crucial. The example of § 3, serves to demonstrate that upper and lower branches can easily be reversed by taking as

ordinate other perfectly natural functionals. KATZ (1978) recognized that certain bifurcation diagrams contain more information than others. His work is discussed further in § 7.

(3) Expression (2.9) is the simplification of a more general formula that is valid in non-variational problems, see for example CRANDALL & RABINOWITZ, (1973), KELLER (1977), or the factorization theorems appearing in IOOSS & JOSEPH (1980), and JOSEPH (1979). However, the more general case contains no natural identification of upper and lower branches. Consequently in a non-variational problem, although it can be proved that an eigenvalue crosses through zero at foldpoint, the direction of the crossing is not immediately available.

(4) Throughout this work the branch $(u(s), \lambda(s))$ and functional $F(u, \lambda)$ are assumed to be smooth, and no attempt is made to state minimal regularity assumptions explicitly. The underlying motivation for this omission is that the validity of each proof is best verified in the context of particular examples. For example, the proof of Proposition 2.1 is valid provided all the derivatives that are written down exist and are continuous.

Now consider solution branches with two successive simple folds. Two such folds necessarily open in opposite directions. If the bottom branch of one fold connects to the top branch of the other, the curve will be described as *s-shaped* (*cf.* Fig. 2 b). If the two top (or two bottom) branches are connected the curve will be called a *spiral.*

Proposition 2.2. *Consider a solution branch in a $-F_\lambda$ vs. λ bifurcation diagram that has two successive simple folds. As a spiral branch is traversed the eigenvalues crossing zero at the folds move in the same direction. As an s-shaped branch is traversed the eigenvalues cross in opposite directions.*

Proof. Two applications of the proof of Proposition 2.1. □

Proposition 2.1 and 2.2 describe the behavior of critical eigenvalues close to simple folds. In order to obtain information far from fold points two further hypotheses are required:

H1: The bifurcation diagram includes all solutions bifurcating from the branch in question.

H2: An eigenvalue cannot cross through zero unless bifurcation occurs.

Hypothesis 1 is a strong requirement, but it is clearly necessary in order that any conclusions can be made. Hypothesis 2 is, on the other hand, very mild. For example, a simple eigenvalue cannot cross unless bifurcation occurs, and in problems with a variational structure, theorems guaranteeing the validity of H2 at multiple eigenvalues are also available. See, for example, CHOW & LAUTERBACH (1985) or ZEIDLER (1984, § 45).

For the moment, the following, somewhat naive, definition will be adopted:

Definition. If eigenvalue problem (2.3) has only positive eigenvalues, the solution (u, λ) will be called *stable.*

Proposition 2.3. *Let* H1 *and* H2 *hold. Consider the spiral and s-shaped branches illustrated in Figure 2, and assume that the folds are simple. Suppose further that*

branch A is stable. Then in the spiral case, branch C has two negative eigenvalues associated with it. In the s-shaped case, branch C is stable.

Proof. The proof employs hypotheses H1 and H2, taken with Proposition 2.2. In the case of the s-shaped branch it should be remarked that as the top fold is traversed upward, an eigenvalue crosses from negative to positive. But only one eigenvalue can do that, namely the lowest one, which becomes negative at the bottom fold. □

Results can also be obtained at nonsimple folds. Notice that the derivation of equations (2.8) and (2.9) is valid provided only that hypothesis (2.6)(c) holds, that is, provided only that the eigenvalue associated with the fold is simple. When either (2.6)(a) or (2.6)(b) fails, identity (2.9) yields the somewhat useless information $\dot{\mu}(s_0) = 0$. However, the analogue of (2.9) that is obtained after repeated differentiation of equation (2.8), demonstrates that the sign at s_0 of the lowest-order nonzero derivative of $\mu(s)$ is determined, by the signs of the lowest-order nonzero derivatives of λ and $-F_\lambda$. Of course, the lowest-order nonvanishing derivative of μ determines the local behavior of μ, and the lowest-order non-vanishing derivatives of λ and $-F_\lambda$ determine the local shape of the solution branch in the $-F_\lambda$ *vs.* λ diagram. Consequently the local shape of the solution branch determines the local behavior of the critical eigenvalue.

For example, suppose that the solution branch in the $-F_\lambda$ *vs.* λ diagram is not a true fold, but is a monotone curve with an isolated vertical tangent, as is depicted in Figure 3. Then the first nonzero derivatives of λ and $-F_\lambda$ must both be of odd order. Moreover, they are of the same sign in the case of Figure 3(a), and of opposite signs in the case of Figure 3(b). Differentiation of (2.8) then implies that the first nonzero derivative of μ is even, and its sign is determined by the signs of the lowest-order derivatives of λ and $-F_\lambda$. Because the first nonzero derivative of μ is of even order, the critical eigenvalue only touches zero at the fold point and does not cross through. The sign of the first nonzero derivative of μ determines whether $\mu(s_0) = 0$ is a local minimum or maximum of $\mu(s)$. The conclusion stated in Figure 3 follows immediately.

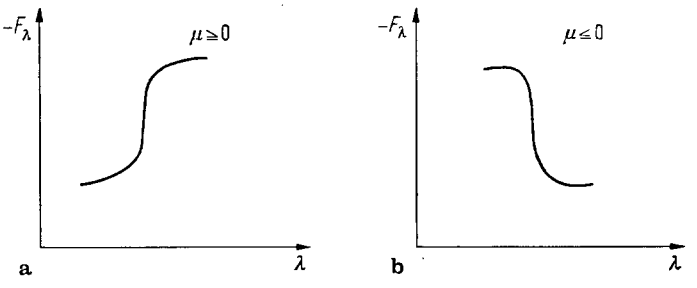

Fig. 3 a and b. Two degenerate fold points

The shape of the solution branch in the $-F_\lambda$ *vs.* λ diagram around a fold point can take many forms. The case most relevant to this development arises in:

Proposition 2.4. *Propositions 2.1, 2.2 and 2.3 remain valid if the hypothesis of a fold being simple is replaced by hypothesis* (2–6)(c), *and the requirement that close to a fold point the solution branch in the* $-F_\lambda$ vs. λ *diagram have the appearance of a simple fold*, viz. *Figure 1.*

Proof. The hypothesis on the shape of the curve is a convenient condition guaranteeing that the first non-vanishing derivative of λ at s_0 is of even order, and that of $-F_\lambda$ is of odd order. Moreover, the sign of the lowest-order non-vanishing derivative of λ is determined by the direction in which the fold opens. Hypothesis (2–6)(c) then suffices to guarantee that the proofs of Propositions 2.1, 2.2 and 2.3 can be followed when equations (2.8) and (2.9) are replaced by their generalizations described above. □

Remarks. (1) In the proof of Proposition 2.4 it is implicitly assumed that the derivatives of some finite order are nonvanishing. In general an analyticity assumption is required to guarantee this property. However analyticity is likely to be too strong a requirement. In any concrete application the failure of some derivative to vanish could be checked directly. (*Cf.* Remark 4 after Proposition 2.1).

(2) Condition (2.6)(b) is the simplification to variational problems of a condition that is sufficient to guarantee isolation of the solution branch through a fold point. See DECKER & KELLER (1981). When (2.6)(b) fails, it is possible for the fold point to be a true bifurcation point. For example, the branch $(u(s), \lambda(s))$ under consideration could be the parabolic part of a simple pitchfork bifurcation. In this case $-\dot{F}_\lambda = 0$, $\ddot{\lambda} \neq 0$, and the stability properties do not alter as the branch is traversed through the fold, or bifurcation, point. Proposition 2.4 is not contradicted because the branch does not have the appearance of a simple fold in the $-F_\lambda$ *vs.* λ diagram: because $-\dot{F}_\lambda$ vanishes and $\ddot{\lambda}$ is nonzero. the solution branch in the $-F_\lambda$ *vs.* λ diagram has a cusp at the fold point. Notice that this lack of smoothness in the projection onto the $-F_\lambda$ vs. λ diagram need not be associated with any lack of smoothness in the solution branch $(u(s), \lambda(s)) \in H \times R$.

If the zero eigenvalue corresponding to the fold has multiplicity $m > 1$, so that condition (2.6)(c) fails, another analogue of (2.9) can be obtained, namely

$$\sum_{k=1}^{m} \alpha_k^2 \dot{\mu}_k = \ddot{\lambda} \frac{d}{ds}\{-F_\lambda\}. \tag{2.10}$$

Here there are m critical eigenvalues μ_k, and m amplitudes α_k, but only one identity involving the derivatives $\dot{\mu}_k$. Expression (2.10) demonstrates that at least one $\dot{\mu}_k$ has the same sign as $\ddot{\lambda}\{\overline{-F_\lambda}\}$, which is sufficient to prove Proposition 2.1 with hypothesis (2–6)(c) omitted. Improved versions of Propositions 2.2, 2.3 and 2.4 are not available. Notice that when the multiplicity is greater than one, there can be several branches with a common fold point (see DECKER & KELLER, 1980). Then equation (2.10) can be derived for each branch, the relevant observation being that the differentiation entailed is with respect to a parametrization of a particular branch.

The above results have been stated in the context of Hilbert space because that setting best reveals the structure of what is essentially a perturbation argu-

ment. In the illustrative examples below, the results of this section are applied without the problems being formulated in Hilbert space. It is a straightforward exercise to rederive the results in the context of each example, but those details are also omitted. One worthwhile remark is that each example is, or is reducible to, a single ordinary differential equation, and consequently it is easy to verify that condition (2.6c) is always satisfied.

§ 3. A Model of Thermal Self-Ignition

Consider the system

$$\begin{aligned} &\Delta u + \lambda^2 e^u = 0, \quad u: \mathscr{B} \subset R^3 \to R, \\ &u|_{\partial\mathscr{B}} = 0, \quad \mathscr{B} \text{ the unit ball.} \end{aligned} \tag{3.1}$$

This equation has a long history; the analysis which we follow is that of GEL'FAND (1963), in which the system is interpreted as a model for thermal self-ignition of a chemically active gas in a spherical vessel. The first analysis of (3.1) is apparently due to ÉMDEN (1907) who considered the equation in an astrophysical context; see also CHANDRASEKHAR (1939) and DAVIS (1962).

Problem (3.1) can, without loss of generality, be reduced to the radial ordinary differential equation

$$\frac{1}{r^2}\frac{d}{dr}r^2\frac{du}{dr} + \lambda^2 e^u = 0, \tag{3.2}$$

$$u'(0) = 0, \quad u(1) = 0, \tag{3.3}$$

and GEL'FAND demonstrates that this system has the bifurcation diagram depicted in Figure 4(a) (see also JOSEPH & LUNDGREN, 1973):

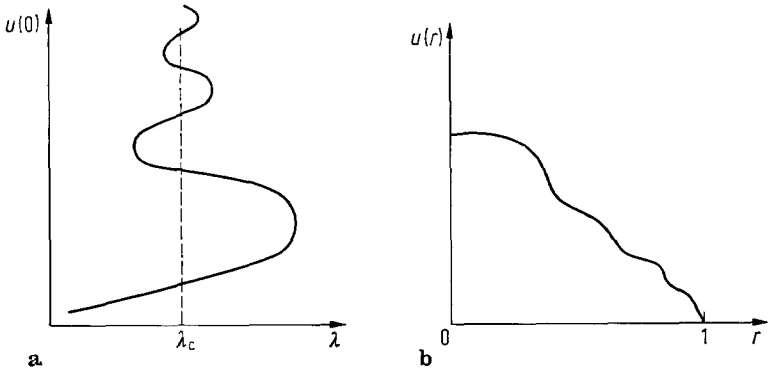

Fig. 4a and b. The bifurcation diagram, and a typical solution associated with system (3.1)

The functional plotted in Figure 4a is $u(0)$, which is the ordinate typically adopted in many similar problems. The bifurcation diagram comprises a single branch with an infinite number of folds centred on a critical value λ_c. For our purposes

the important feature of the solution is that although $u(r)$ is monotone decreasing, $u'(r)$ is oscillatory. The demonstration of these facts depends upon a certain transformation: if $u_0(r)$ is a solution of equation (3.2), so is

$$u(r, \alpha) = \alpha + u_0(r^{\alpha/2}e). \tag{3.4}$$

Consequently, if one solution satisfying $u_0'(0) = 0$ can be found, then the two point boundary-value problem, can be solved by shooting from $r = 0$. We do not repeat all the details here, but refer instead to GEL'FAND (*op. cit.*). The analysis in § 4 below is a simpler example of the same method.

The constant α appearing in (3.4) can be adopted as the parametrization of the solution branch, in which case it is straightforward to verify that all the folds are simple. Moreover Hypothesis 1 and 2 hold.

It remains only to calculate the preferred functional. Because all solutions are radial, equation (3.2) can be obtained as the Euler-Lagrange equation of the functional

$$F(u, \lambda) = \int_0^1 \{\tfrac{1}{2}u'^2 - \lambda^2 e^u\} r^2 \, dr, \quad u'(0) = 0, \quad u(1) = 0.$$

Accordingly, the preferred functional is

$$-F_\lambda = 2\int_0^1 \lambda e^u r^2 \, dr.$$

But integration of (3.2) demonstrates that on solutions

$$\lambda \int_0^1 e^u r^2 \, dr = -\frac{u'(1)}{\lambda}.$$

The analysis of GEL'FAND (*ibid.*, in particular Figure 15, p. 361) demonstrates that the bifurcation diagram with $-F_\lambda$ as ordinate has the qualitative form shown in Figure 5, namely an infinite spiral. The results of § 2 apply, and provide the information that as the spiral is traversed inward, an eigenvalue crosses from the positive to the negative half-line at each successive fold. Thus the only possible stable region is the lowest segment of the branch, and it is easily verified that that region is indeed stable. This example demonstrates that

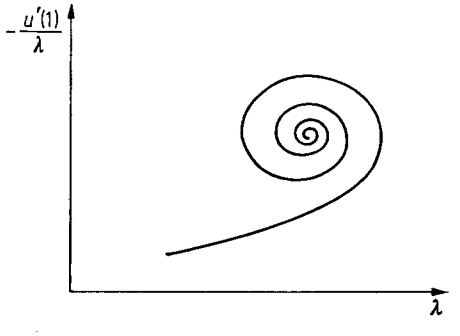

Fig. 5. The preferred bifurcation diagram for system (3.1)

the property of a branch being spiral or s-shaped in a bifurcation diagram is not preserved under change between two simple and natural ordinates. Stability predictions can only be fully made from the $-F_\lambda$ *vs.* λ diagram.

§ 4. A Model of a Chemical Reactor

Consider the following boundary-value problem, which is of Émden-Fowler type:

$$u_{xx} = \phi^2 u^p, \quad p < -1, \quad u(x) > 0, \tag{4.1}$$

$$u_x(0) = 0, \quad u(1) = 1. \tag{4.2}$$

This system is a model for the steady-state solutions of a reaction-diffusion system governing the concentration $u(x)$ of a substance disappearing according to a p^{th} order isothermal reaction in an infinite slab of catalyst. Further details can be found in MEHTA & ARIS (1971). In this and analogous problems appearing in the chemical engineering literature, the bifurcation parameter ϕ is known as the Thiele modulus. The delimitation on the range of the parameter p is not physically required, but the other cases are not such suitable illustrations of the theory developed in this paper.

The complete set of solutions to (4.1) and (4.2) can be obtained straightforwardly in a standard way. First change the independent variable to $t = \phi x$, to obtain the boundary-value problem

$$u_{tt} = u^p, \quad u_t(0) = 0, \quad u(\phi) = 1, \tag{4.2}$$

and define $y(t)$ to be the solution of the initial-value problem

$$y_{tt} = y^p, \quad y_t(0) = 0, \quad y(0) = 1. \tag{4.3}$$

Then for any positive constant A

$$u(t, A) = A^\beta y(At), \quad \beta = 2/(p-1) \tag{4.4}$$

is a solution of

$$u_{tt} = u^p, \quad u_t(0) = 0, \quad u(0) = A^\beta. \tag{4.5}$$

Accordingly, boundary-value problem (4.2) can be solved by shooting from $t = 0$, while scanning all positive values of A. This procedure defines a one-parameter family of curves in the (u, t) plane; the envelopes of that family are determined next.

Any envelope $e(t)$ is of the form

$$e(t) = u(t, A(t)) = A^\beta(t)\, y(A(t)\, t), \tag{4.6}$$

where the function $A(t)$ is defined by the condition

$$0 = \beta A^{\beta-1}\, y(At) + A^\beta t y'(At) \left[= \frac{\partial}{\partial A} A^\beta y(At) \right]. \tag{4.7}$$

Accordingly,

$$A(t) = \frac{S}{t}, \quad \text{and} \quad e(t) = \frac{S^\beta}{t^\beta} y(S), \tag{4.8}$$

where the constant S is any positive root of

$$\beta y(S) + S y'(S) = 0. \tag{4.9}$$

But the left-hand side of (4.9), when regarded as a function of S, has derivative

$$(1 + \beta) y' + S y'' = (1 + \beta) y' + S y^p, \tag{4.10}$$

which is strictly positive because

$$-1 < \beta < 0 \quad \text{and} \quad y' > 0. \tag{4.11}$$

As the left-hand side of (4.9) is negative at $S = 0$, it may be concluded that (4.9) has a unique root.

Members of the family of solutions (4.4) are sketched in Figure 6. Let the number ϕ^* satisfy

$$e(\phi^*) = 1. \tag{4.12}$$

Then for $\phi < \phi^*$, $\phi = \phi^*$, and $\phi > \phi^*$, boundary-value problem (4.1), (4.2) has, respectively, two, one and no solutions. In the case of $\phi < \phi^*$, one solution touches the envelope for $t < \phi$, and the other for $t > \phi$.

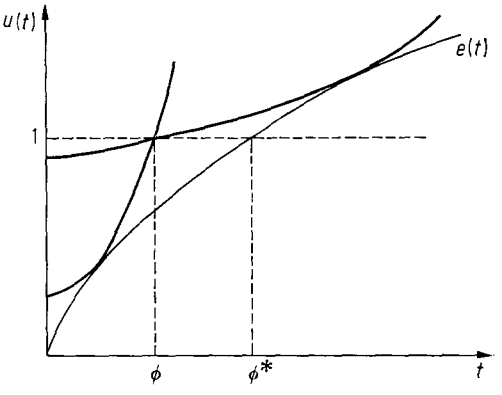

Fig. 6. Two solutions and the envelope of initial value problem (4.3)

Consideration of Figure 6 demonstrates that system (4.1) and (4.2) has the bifurcation diagram depicted in Figure 7. That is, for each value of p the bifurcation diagram comprises a single fold, and the folds for differing values of p are nested.

In the context of chemical engineering it is usual to introduce a functional $\eta(u)$ called the *effectiveness factor* that is defined by

$$\eta(u) = \int_0^1 u^p \, ds. \tag{4.13}$$

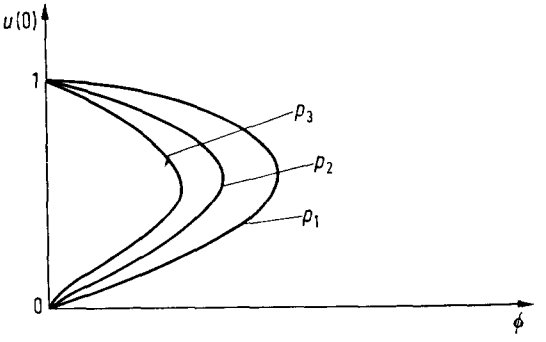

Fig. 7. Bifurcation diagrams for system (4.1) and (4.2), with three values of p, $p_1 > p_2 > p_3$

On solutions

$$\eta(u) = \frac{1}{\phi^2} u_x(1). \tag{4.14}$$

The following fact will be used later in the development: at the fold point the value of η, η^* say, is given by the formula

$$\eta^* = \frac{-\beta}{\phi^{*2}}, \quad \beta = \frac{2}{(p-1)}. \tag{4.15}$$

This last expression can be derived from (4.8), (4.12) and (4.14), because whenever $\phi = \phi^*$ the solution and the envelope osculate at $t = 1$.

Equation (4.1) is the Euler-Lagrange equation for the functional

$$\int_0^1 \left\{ \tfrac{1}{2} u_x^2 + \frac{\phi^2}{p+1} u^{p+1} \right\} dx$$

and ϕ^2 may be regarded as the bifurcation parameter rather than ϕ itself. Then the preferred functional $-F_\lambda$ is

$$-\frac{1}{(p+1)} \int_0^1 u^{p+1}\, dx. \tag{4.16}$$

Now, integration of (4.1), after multiplication by u, provides the relation

$$\phi^2 \int_0^1 u^{p+1}\, dx = \int_0^1 u u_{xx}\, dx = u_x(1) - \int_0^1 u_x^2\, dx. \tag{4.17}$$

But equation (4.1) has the first integral

$$\tfrac{1}{2} u_x^2(x) = \frac{\phi^2}{(p+1)} (u^{p+1}(x) - u^{p+1}(0)). \tag{4.18}$$

Upon setting $x = 1$ in (4.18), we obtain

$$\eta^2 = \frac{2}{\phi^2(p+1)} (1 - u^{p+1}(0)). \tag{4.19}$$

Furthermore integration of (4.18) yields

$$\frac{\phi^2}{(p+1)}\int_0^1 u^{p+1}\,dx = \tfrac{1}{2}\int_0^1 u_x^2\,dx + \frac{\phi^2}{(p+1)}u^{p+1}(0), \tag{4.20}$$

and, upon combining (4.14), (4.17), (4.19) and (4.20), we obtain

$$\left(\frac{p+3}{p+1}\right)\int_0^1 u^{p+1}\,dx = \eta - \phi^2\eta^2 + \frac{2}{(p+1)}. \tag{4.21}$$

That is, for the system (4.1), (4.2) with $p \neq -3$, or -1, the $(p+1)^{\text{th}}$ power of the L^{p+1} "norm" of any solution can be expressed as a simple quadratic function of the p^{th} power of its L^p "norm". In particular, for $p \neq -3$ or -1, equation (4.21) expresses the functional $-F_\lambda$ in terms of the effectiveness factor η.

In light of identity (4.21) the theory developed in § 2 can be applied without explicitly constructing the preferred bifurcation diagram; it suffices to plot the η *vs.* ϕ^2 diagram. This was done numerically by MEHTA & ARIS (*op. cit.*). For our purposes all that is required is the qualitative form of the folds, which information is deducible analytically, combined with the result expressed in equation (4.15).

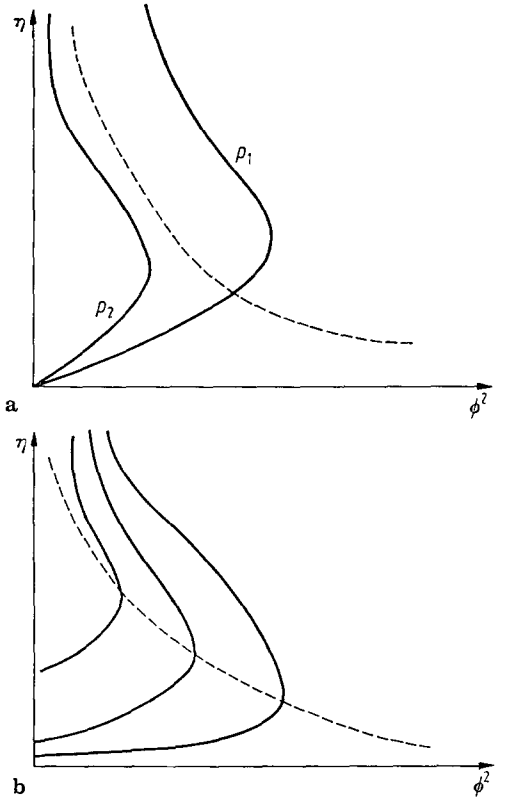

Fig. 8a. Bifurcation diagram for system (4.1) and (4.2) with effectiveness η as ordinate, $p_2 < -3 < p_1$; b level sets of the function $\eta - \phi^2\eta$

The η *vs.* ϕ^2 diagram is drawn in Figure 8 a; the solid lines represent solution branches, and the dashed line is the curve $\eta = \frac{1}{2}\phi^2$. In Figure 8 b the level sets of the function $\eta - \phi^2\eta$, have been plotted, with the curve $\eta = \frac{1}{2}\phi^2$, again being shown. This last curve is the locus on which the level sets of $\eta - \phi^2\eta^2$ have vertical tangents; above that line the level sets have negative slope; below that lines the level sets have positive slope.

Now equation (4.15) states that when $-3 < p < -1$ the fold point lies above the line $\eta = \frac{1}{2}\phi^2$, and when $p < -3$ the fold point lies below the line. Accordingly, due to the form of the level sets, it can be seen that as a fold in the η *vs.* ϕ^2 diagram is traversed upward, the function $\eta - \phi^2\eta$ decreases or increases as $p > -3$ or $p < -3$, respectively. But because the factor $p + 3$ appears in (4.21) the functional $-F_\lambda$ increases in either case. Thus the top branch in the η *vs.* ϕ^2 diagram is unstable provided $p \neq -3$. Notice that the upper branches in the η *vs.* ϕ^2 diagram correspond to the lower branches in the $u(0)$ *vs.* ϕ^2 diagram.

The above analysis does not apply when $p = -3$, but the top branch in the η *vs.* ϕ^2 diagram is also unstable in this case. This fact is readily verified because when $p = -3$, (4.1) and (4.2) have the simple solution

$$u(x)^2 = \frac{\phi^2}{u(0)^2}x^2 + u(0)^2,$$

where $u(0)^2 = \frac{1}{2} \pm \sqrt{\frac{1}{4} - \phi^2}$. There are two branches which exist for $\phi^2 \leqq \phi^{*2} = \frac{1}{4}$, and explicit formulas for η and $-F_\lambda$ can be obtained.

The example of this section demonstrates that the qualitative features of the $-F_\lambda$ *vs.* λ diagram that must be known to predict stability transitions, may be deducible from another bifurcation diagram.

§ 5. Isoperimetric Problems

Suppose that the functional $F(u, \lambda)$ has the special form

$$F(u, \lambda) = G(u) - \lambda H(u), \qquad (5.1)$$
$$\lambda \in R, \quad G, H: \mathscr{H} \to R.$$

This case is of interest for two reasons; firstly, problems in mechanics are often of this type, and secondly, this form encompasses two interpretations, an unconstrained problem as before, or an isoperimetric problem.

The simplest isoperimetric problem is

$$\min_u G(u) \quad \text{subject to } H(u) = C, \qquad (5.2)$$

where C is a given constant. The theory of Lagrange multipliers asserts that the first-order conditions for problem (5.2) coincide with those of

$$\min_u \{G(u) - \lambda H(u)\}. \qquad (5.3)$$

That is, the extremals of both problems satisfy an Euler-Lagrange equation

$$G' - \lambda H' = \mathbf{0}. \qquad (5.4$$

Consequently, an extremal of (5.3) for given λ is also an extremal of (5.2) for some C, and *vice versa*; the set of extremals in an H *vs.* λ diagram is the same for both problems. In the isoperimetric case $H(u)$ is specified and the possible values of λ are determined by use of (5.4), whereas in the unconstrained problem λ is specified and the possible values of $H(u)$ are determined through (5.4).

The theory of § 2 relates the shape of the solution branch in the H *vs.* λ diagram to the question of whether the extremal is a local minimum. In the case where λ enters linearly another result is available, namely

Lemma 5.1. *Suppose that* (u, λ) *is a stable solution of* (5.3). *Then the slope of the solution branch at* (u, λ) *in the* H vs. λ *diagram is non-negative.*

Proof. Differentiate (5.4), and take the innerproduct with $\dot{u}$ to obtain

$$\langle \dot{u}, \{G'' - \lambda H''\}\, \dot{u}\rangle = \dot{\lambda}\langle H', \dot{u}\rangle = \dot{\lambda}^2 \frac{d}{d\lambda} H.$$

But as the branch is assumed stable, the left hand side is non-negative. □

The analogous results for *constrained* local minima are now developed. Although the sets of extremals for the constrained and unconstrained problems coincide, the second-order conditions for an extremal to be a constrained or unconstrained minimum differ. The necessary second-order condition in the isoperimetric problem is that the second variation be non-negative on the tangent space to the constraint surface $H(u) = C$. If (u, λ) denotes a constrained extremal, this condition can be written as

$$\langle \eta, \{G''(u) - \lambda H''(u)\}\, \eta\rangle \geqq 0, \quad \forall \eta \neq 0 \text{ such that } \langle H'(u), \eta\rangle = 0. \tag{5.5}$$

Here $H'(u) \in \mathscr{H}$ is the first Fréchet derivative of H at u, and $G''(u)$ and $H''(u)$ are the linear self-adjoint operators $\mathscr{H} \to \mathscr{H}$ that are the second Fréchet derivatives of G and H. For brevity we shall introduce the notation

$$L(u, \lambda) = G''(u) - \lambda H''(u). \tag{5.6}$$

We shall determine when (5.5) holds with a sharp inequality. Condition, (5.5) with strict inequality will be referred to as condition (5.5)′. Recall the analogous unconstrained condition, (2.3) which can be rewritten as:

$$\text{all eigenvalues of } L\eta = \mu\eta, \quad \eta \in \mathscr{H},\ \mu \in R \text{ are positive.} \tag{5.7}$$

Conditions of the form (5.5)′ have been analyzed by many authors. Here we shall exploit some elementary observations and obtain a Lemma.

Remarks. (1) Unless $H'(u)$ happens to be an eigenfunction of L, condition (5.5)′ cannot be stated solely in terms of the eigenvalues of L.

(2) If condition (5.7) holds, then condition (5.5)′ holds.

(3) If L has two non-positive eigenvalues then (5.5)′ fails.

Lemma 5.2. *Suppose that on some segment of the solution branch,* L *is non-singular and has precisely one negative eigenvalue. Then condition* (5.5)′ *holds if and only if the slope of the branch at* (u, λ) *in the* H vs. λ *diagram is negative.*

Proof. Provided that L has precisely one negative eigenvalue, the theory described in MADDOCKS (1985) (see also the simpler proof described in MADDOCKS, 1984, p. 352) simplifies to state that (5.5)′ holds if and only if

$$\langle \xi, L\xi \rangle < 0,$$

where ξ is defined to be the solution of

$$L(u)\,\xi = H'(u).$$

But differentiation of (5.4) shows that

$$\xi = \dot{u}/\dot{\lambda},$$

and

$$\langle \xi, L\xi \rangle = \frac{\langle H', \dot{u} \rangle}{\dot{\lambda}} = \frac{dH}{d\lambda}.$$

Notice that as L is assumed to be nonsingular

$$\dot{\lambda} \neq 0.$$

□

Remarks 1–3 and Lemma 5.2 can be summarized as follows. As before an extremal will be called stable if condition (5.7) holds; an extremal will be called c-stable if condition (5.5)′ holds. All stable extremals are c-stable. The set of extremals that are c-stable, but not stable, is the union of those extremals on which L has precisely one negative eigenvalue and $\frac{dH}{d\lambda}$ is negative, and some exceptional extremals on which L is singular.

Consider as an example the H *vs.* λ diagrams drawn in Figure 9. Suppose that the folds are simple, that hypotheses H1 and H2 hold and that in each case branch A is stable. Then in case (a) the results of § 2 imply that segment E is stable, and segments B, C and D are unstable. The results of this section give the further information that segments B and D are c-stable, but that segment C is not c-stable. In case (b), A is the only stable segment, and A and B are the only c-stable segments. Segment D has two associated negative eigenvalues, so that it can be neither stable nor c-stable. Notice that c-stability is lost or gained at horizontal folds.

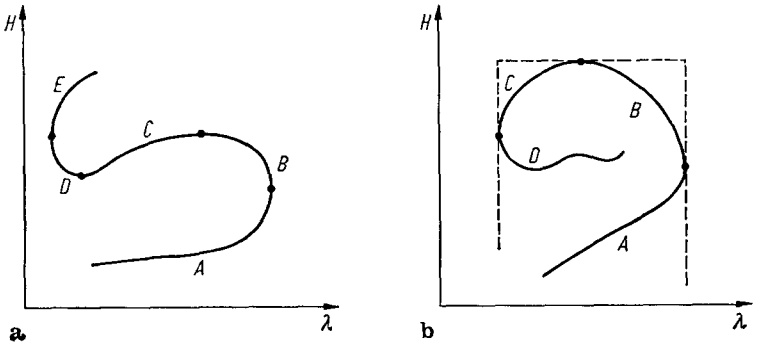

Fig. 9a and b. Possible bifurcation diagrams. The labelled segments have boundaries at the points with vertical and horizontal tangents

Examples in elasticity with uniaxial loading comprise one important class of problems that have the structure of (5.3). In this case λ represents the magnitude of a load, $H(u)$ is a displacement, and $G(u)$ is the elastic stored energy. The example analyzed in § 6 is of this type. The unconstrained problem in which the load λ is specified is known as *dead loading*, and the isoperimetric problem in which the displacement $H(u)$ is specified is known as *hard loading*. In either case, the theory here presented allows stability predictions to be made from the shape of the solution branch in the H vs. λ diagram. But this diagram is the load-displacement graph (actually the displacement-load graph), which is commonly computed or measured in experiments.

It should be emphasized that load-displacement and stress-strain diagrams are almost always distinct objects. Confusion frequently arises over this point, perhaps because in the basic example of uniform extension of a one-dimensional bar (see *e.g.* ERICKSEN, 1975), the response curve in the load-displacement graph and the constitutive curve in the stress-strain diagram, happen to be identical. The confusion is exacerbated by the fact that there are instability results associated with non-monotone stress-strain curves; for example, Legendre's condition in the calculus of variations can often be viewed in this light. Non-monotonicity of the stress-strain law is associated with a loss of ellipticity in the linearized problem. The accompanying instability results are of a nature entirely different from that of the instability results developed here, which are associated with non-monotonicity of the load-displacement graph. The analysis of the next section provides an example in which the stress-strain curve is monotone, but the load-displacement graph is non-monotone.

§ 6. A Model of a Cantilever

In this section we shall analyze the following problem:

$$\min \int_0^1 \{W(\phi_s) + \lambda \cos \phi\}\, ds,$$
$$\phi(0) = \alpha, \quad 0 \leqq \alpha \leqq \frac{\pi}{2}, \quad \lambda \geqq 0. \tag{6.1}$$

This example can be interpreted as a model determining the equilibrium configurations of a uniform elastic rod when subject to cantilever loading. The situation envisaged is illustrated in Figure 10. The parameter λ is the force applied to the end $s = 1$ of the rod. Specification of λ corresponds to dead loading. Specification of the distance l corresponds to hard loading, in which case λ enters as a Lagrange multiplier and the condition

$$\int_0^1 \cos \phi\, ds = l, \quad |l| < 1, \tag{6.2}$$

must be added to (6.1).

The function $W(p): R \to R^+$ is the strain energy density function, which is determined by constitutive properties of the rod. We shall assume that W is

smooth and satisfies

$$W(0) = 0 \quad \text{(i)}, \qquad W'(0) = 0 \quad \text{(ii)}, \qquad W''(p) > 0, \forall p \quad \text{(iii)},$$
$$W''(0) = 1 \quad \text{(iv)}, \qquad W/|p| \to \infty \text{ as } p \to \infty \quad \text{(v)}, \tag{6.3}$$
$$W(p) = W(-p), \forall p \quad \text{(vi)},$$

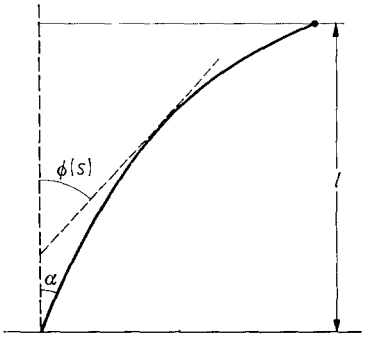

Fig. 10. The system analyzed in § 6. An elastic rod is cantilevered at one end, *i.e.* $\phi(0)$ is specified. The other end is free to move horizontally, and no moment is applied, but vertical loading is present. In the case of dead-loading a vertical force λ is prescribed, in the case of hard-loading the distance l is prescribed

which are all standard hypotheses. Conditions (i), (iv) and (vi) are merely conveniences. Condition (ii) is the statement that the unstressed state of the rod is straight. The condition $W'(p^*) = 0$ for $p^* \neq 0$ would correspond to an arc of a circle as the unstressed state. The methods of the subsequent analysis can also be applied to that case, which is of some importance in designing leaf springs. The only change in formulation is in the natural boundary condition (6.5) below. Conditions (iii) and (v) are crucial; they are the statements that the stress-strain curve is monotone, and that infinite strain implies infinite stress. We shall contrast possible behavior depending on whether or not the additional constitutive assumption

$$W''(p) \geqq \frac{W'(p)}{p}, \quad \forall p, \tag{6.4}$$

is made.

The first-order conditions for extremals of (6.1) are the natural boundary condition

$$\phi_s(1) = 0 \tag{6.5}$$

and the DuBois-Reymond equation, which is the first integral of the Euler-Lagrange equation of (6.1),

$$\phi_s W' - W = \lambda(\cos\phi - \cos\gamma), \tag{6.6}$$

where $\gamma = \phi(1)$. Equation (6.6) has the phase-plane drawn in Figure 11 a. Extremals of (6.1) correspond to trajectories in the phase-plane that intersect the line $\phi = \alpha$ when $s = 0$, and intersect the line $\phi_s = 0$ when $s = 1$. Accor-

dingly the problem is reduced to determining which of those trajectories satisfying the boundary conditions also have the correct arc-length.

The first step is to invert (6.6) and solve for ϕ_s; hypotheses (6.3)(iii) and (v) ensure that this can be done. Equation (6.6) can be written in the form

$$\phi_s^2 = g(\lambda(\cos\phi - \cos\gamma)),$$

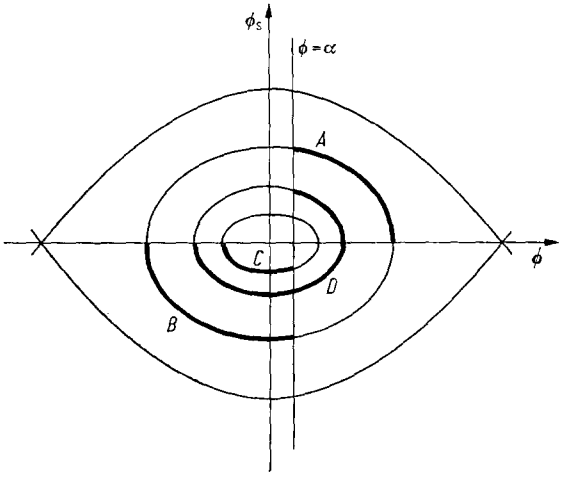

Fig. 11a. Phase plane of equation (6.6)

that is $pW'(p) - W$ is regarded as a function $F(p^2)$, and g is the inverse of F. Then

$$\phi_s = \frac{\{\lambda(\cos\phi - \cos\gamma)\}^{\frac{1}{2}}}{f(\lambda(\cos\phi - \cos\gamma))}, \tag{6.7}$$

where the function $f(x)$ is defined by

$$f(x) = \{x/g(x)\}^{\frac{1}{2}}. \tag{6.8}$$

The constitutive hypotheses (6.1) translate into conditions on the function f. In particular,

$$\begin{aligned} &f(x) \to 1/\sqrt{2} \\ &f'(x) \to 0 \end{aligned} \quad \text{as } x \to 0, \quad \text{(i)}$$

$$f - 2xf' > 0 \quad \forall x > 0, \quad \text{(ii)} \tag{6.9}$$

$$f^2/x \to 0 \quad \text{as } x \to \infty \quad \text{(iii)}$$

and

$$f > 0 \quad \forall x > 0. \quad \text{(iv)}$$

Furthermore, condition (6.4) becomes

$$f' \geqq 0 \quad \forall x > 0. \tag{6.10}$$

The prototypical example is that of linear elasticity in which $W(p) = \frac{1}{2}p^2$ and $f(x) \equiv 1/\sqrt{2}$.

Due to the symmetry present in the problem, the arc-length associated with any relevant trajectory can be computed from the integrals

$$L_1(\gamma, \lambda) = \int_0^{\alpha} \frac{d\phi}{\phi_s} = \int_0^{\alpha} \frac{f(\lambda(\cos\phi - \cos\gamma))}{\{\lambda(\cos\phi - \cos\gamma)\}^{\frac{1}{2}}} d\phi, \tag{6.11}$$

and

$$L_2(\gamma, \lambda) = \int_0^{\gamma} \frac{d\phi}{\phi_s} = \int_0^{\gamma} \frac{f(\lambda(\cos\phi - \cos\gamma))}{\{\lambda(\cos\phi - \cos\gamma)\}^{\frac{1}{2}}} d\phi. \tag{6.12}$$

The following properties of the functions L_1 and L_2 allow us to obtain the pertinent bifurcation diagrams:

Lemma 6.1. *(Monotonicity properties leading to existence results.)*

$$\text{(i)} \quad \frac{\partial L_1}{\partial \lambda} < 0, \quad \frac{\partial L_2}{\partial \lambda} < 0, \quad \frac{\partial}{\partial \lambda}(L_2 - L_1) < 0. \tag{6.13}$$

$$\text{(ii)} \quad \frac{\partial L_1}{\partial \gamma} < 0, \quad \text{and} \quad \lim_{\gamma \to \alpha, \pi} L_1 \text{ is finite.} \tag{6.14}$$

(iii) $(L_1 + L_2)(\gamma, \lambda)$ *for fixed* λ *has a minimum at* $\gamma = \gamma^*(\lambda) > \alpha$.

$$\text{(iv)} \quad \lim_{\gamma \to \pi} L_2 = +\infty, \quad \text{and} \quad \lim_{\gamma \to 0} L_2 = \frac{\pi}{2\sqrt{\lambda}}. \tag{6.15}$$

$$\text{(v)} \quad \textit{If condition (6.10) holds,} \quad \frac{\partial}{\partial \gamma} L_2 > 0. \tag{6.16}$$

The proofs are effected by straightforward but lengthy computation, and use of (6.9)(ii). The function $L_2(\gamma, \lambda)$ has the same structure as an elliptic integral, and consequently calculations are much simplified if the transformation

$$\sin\frac{\gamma}{2} \sin\psi = \sin\phi/2 \tag{6.17}$$

is introduced. Then

$$L_2(\gamma, \lambda) = \sqrt{\frac{2}{\lambda}} \int_0^{\pi/2} \frac{f(2\lambda a \cos^2\psi)}{\{1 - a\sin^2\psi\}^{\frac{1}{2}}} d\psi \tag{6.18}$$

where $a = \sin^2\frac{\gamma}{2}$. □

Remark 1. The limit (6.15) as $\gamma \to 0$ is the lowest Euler-Bernoulli buckling load.

Remark 2. If condition (6.10) does not hold, $\frac{\partial L_2}{\partial \gamma}$ need not be of one sign.

For example, $f(x)$ can be chosen to be a smooth mollification of a monotone decreasing stepfunction for which hypotheses (6.3) on the associated W are satisfied, and each jump gives rise to a change of sign in $\dfrac{\partial L_2}{\partial \gamma}$.

Consider problem (6.1) with $\alpha = 0$. This is the classic buckling problem which has antecedents in the works of EULER. The bifurcation diagram has the form sketched in Figure 11 b. The trivial solution exists for all loads λ and buckled solutions bifurcate at the Euler-Bernoulli loads

$$\lambda = \frac{(2n+1)^2 \pi^2}{4}, \quad n = 0, 1, 2, \ldots$$

Of course, the first mode makes a quarter turn around the origin in the phase-plane of (6.6), the second a three-quarters turn, *etc.* Monotonicity properties (6.13) demonstrate that $\gamma = \phi(1)$ can be used as a parametrization of each buckled branch. This is because each value of γ must have precisely one value of λ such that $L_2(\gamma, \lambda) = 1$. However, whenever L_2 is not monotone in γ there will be values of λ for which $L_2(\gamma, \lambda) = 1$ has multiple roots and the buckled branch will be folded, as is drawn in Figure 11 b.

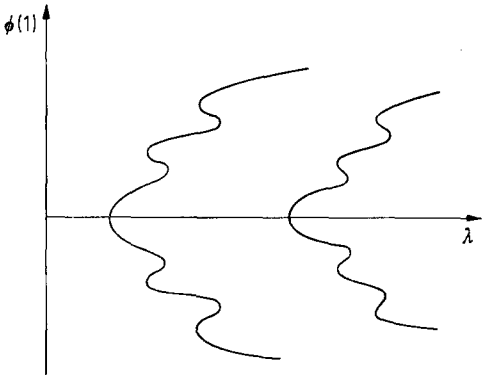

Fig. 11 b. Bifurcation diagram for (6.1) when $\alpha = 0$

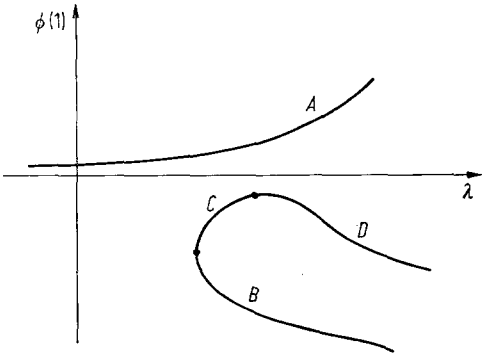

Fig. 11 c. Bifurcation diagram for (6.1) with $\alpha > 0$, and (6.4) valid

In the case $\alpha > 0$, the bifurcation diagram drawn in Figure 11(c) is obtained. Here it has been assumed for simplicity that constitutive hypothesis (6.4), or equivalently (6.10) holds. Otherwise further folds could be present .Typical phase-plane trajectories corresponding to solutions in the segments A, B, C and D of the bifurcation diagram are labelled in Figure 11 a. When $\alpha \neq 0$ there is no trivial solution, but there is a *primary* branch that exists for all $\lambda > 0$, and which corresponds to trajectories in the phase-plane making less than a quarter turn. The fold point on the secondary branch corresponds to the value of λ at which $(L_1 + L_2)(\lambda, \gamma^*(\lambda)) = 1$ (see Lemma 6.1 (iii) for the definition of $\gamma^*(\lambda)$). Notice that although Figure 11 c is an unfolding of Figure 11 b, there no assumption of smallness of α in this analysis.

Stability properties of the various branches are now considered. To this end, note that

$$H(\phi) = -\int_0^1 \cos\phi \, ds. \tag{6.19}$$

The following lemmas will be assumed:

Lemma 6.2. *(Monotonicity properties leading to stability results.)*
Define

$$Q_1(\gamma, \lambda) = \int_0^{\alpha} \frac{\cos\phi}{\phi_s} d\phi = \int_0^{\alpha} \frac{\cos\phi \; f(\lambda(\cos\phi - \cos\gamma))}{\{\lambda(\cos\phi - \cos\gamma)\}^{\frac{1}{2}}} d\phi, \tag{6.20}$$

and

$$Q_2(\gamma, \lambda) = \int_0^{\gamma} \frac{\cos\phi}{\phi_s} d\phi = \int_0^{\gamma} \frac{\cos\phi \; f(\lambda(\cos\phi - \cos\gamma))}{\{(\cos\phi - \cos\gamma)\}^{\frac{1}{2}}} d\phi. \tag{6.21}$$

Then

$$\text{(i)} \quad \frac{\partial L_1}{\partial\lambda} < \frac{\partial Q_1}{\partial\lambda} < 0; \quad \frac{\partial L_2}{\partial\lambda} < \frac{\partial Q_2}{\partial\lambda} < 0; \quad \frac{\partial(L_2 - L_1)}{\partial\lambda} < \frac{\partial(Q_2 - Q_1)}{\partial\lambda} < 0, \tag{6.22}$$

$$\text{(ii)} \quad \frac{\partial L_1}{\partial\gamma} < \frac{\partial Q_1}{\partial\gamma} < 0; \quad \text{and} \quad \frac{\partial Q_2}{\partial\gamma} < \frac{\partial L_2}{\partial\gamma}. \tag{6.23}$$

Proof. By laborious calculation. The derivative of (6.23) employs transformation (6.17), and one integration by parts. □

Lemma 6.3. *A solution of* (6.1) *with n interior zeroes of the function ϕ_s has at most $(n + 1)$ associated negative eigenvalues.*

Proof. A straightforward applicatlon of conjugate point theory, and Sturm comparison theory. Similar arguments can be found in MADDOCKS (1984).

Proposition 6.1. *Let* $\alpha = 0$. *Then on the branch representing the first buckled mode, the forward going segments,* i.e. *those segments for which* $\frac{d\phi(1)}{d\lambda} > 0$, *are stable, and the backward portions are unstable under dead loading. The whole of the first branch is stable under hard loading.*

Proof. The assertion of dead loading stability is essentially standard. By Lemma 6.3 the first mode has at most one negative eigenvalue. Accordingly any series of folds must involve successive losses and recoveries of stability. The theory of § 2 applies to reaffirm this conclusion, because we shall show that $H(\phi)$ increases monotonically as the branch is traversed outward.

The theory of § 5 is required to obtain the conclusions concerning hard loading. But given Lemma 5.2, the result is immediate from the monotonicty of $H(\phi)$ along the branch. To prove this monotonicity property recall that γ is a parametrization of the branch. Moreover,

$$-\frac{d}{d\gamma} H(\phi) = \frac{d}{d\gamma} Q_2(\gamma, \lambda(\gamma)) = \frac{\partial Q_2}{\partial \gamma} + \frac{\partial Q_2}{\partial \gamma}\frac{d\lambda}{d\gamma}.$$

Consider a backward segment, so that $\frac{d\lambda}{d\gamma} \leqq 0$. Then inequalities (6.22)(b) and (6.23)(b) imply that

$$\frac{\partial Q_2}{\partial \gamma} + \frac{\partial Q_2}{\partial \lambda}\frac{d\lambda}{d\gamma} < \frac{\partial L_2}{\partial \gamma} + \frac{\partial L_2}{\partial \lambda}\frac{d\lambda}{d\gamma} = 0, \tag{6.24}$$

the last equality arising because $L_2(\gamma, \lambda(\gamma))$ is constant on the branch. Inequality (6.24) demonstrates that H increases with γ at each fold-point and on backward going segments, which combined with Lemma 6.3 is sufficient to complete the proof. A direct proof that Q_2 is also monotone on forward going segments of the first buckled branch is not immediately available, but this monotonicity property is a consequence of Lemma 5.1. □

Proposition 6.2. *Let* $0 < \alpha \leqq \frac{\pi}{2}$. *Then the forward going segments of the primary branch (branch A in Figure 12 b) are stable, and any backward portions are unstable under dead loading. The whole of the primary branch is stable under hard loading.*

Proof. The method of the proof of Proposition 6.2 can be applied to the functional $Q_2 - Q_1$. □

It is physically clear that for λ sufficiently large, $\frac{dH}{d\lambda}$ is negative on both segments B and D of the secondary branch of solutions (*cf.* Figure 11 c). Moreover, the forward going portions of branch B are stable. Consequently, the secondary branch provides an example in which constrained stability is lost at a point of horizontal tangency in the H *vs.* λ diagram. However, a detailed analysis is complicated, and the issue is not pursued here.

§ 7. Discussion

The thesis here presented is that bifurcation problems with variational structure possess a natural bifurcation diagram that contains the maximum possible amount of information concerning the stability properties of solutions. This distinguished diagram is defined by specification of a particular functional that should be plotted as ordinate. That any functional should be so adopted is a somewhat disputable point; many authors prefer schematic bifurcation diagrams in which the ordinate represents a function space. This last approach has the advantage that symmetries in the solution set can easily be indicated. Nevertheless, if stability properties of a folded branch are the main concern, the best choice of bifurcation diagram is the one described in § 2.

Theorems connecting the shape of solution branches with stability properties have a long history dating back at least to POINCARÉ. That literature is not reviewed here; only those works bearing directly on these results are mentioned. The main feature demarcating this presentation from the body of the literature is that stability of an immediately adjacent branch is not taken as a hypothesis. Consequently this theory is particularly useful on branches with a succession of folds.

Another distinguishing feature is that this theory depends only on the shape of one branch close to a fold point; the presence or absence of adjacent branches is not exploited. The ramifications of this fact have yet to be fully explored. In particular, it remains to determine whether a variational structure allows an improvement to be made in the usual theory concerning stability exchanges at bifurcation points (see MADDOCKS & JEPSON, 1986).

The results presented here are not new in their entirety. Rather, the claim is that a considerable unification and extension of previous work is achieved. The theory has antecedents both in the mathematical literature, and in more applied fields. The most relevant mathematical works were cited in Remark 3 of § 2; many of those authors obtain the non-variational analogue of formula (2–9), but the remaining analysis cannot be completed in the more general case.

KATZ (1978, 1979) realized the significance of a particular bifurcation diagram to stability predictions in variational problems. He considered the minimization of a function $F(x_1, \ldots, x_n, \lambda)$ depending on n coordinates x_i, and a parameter λ, and proved the equivalent of the restriction to finite dimensions of Proposition 2.1. His proof was based on the assumption that the equilibrium conditions can be cast as a diagonal matrix equation. The method does not generalize to non-simple folds in any obvious manner. KATZ applies his results to various examples from astrophysics.

THOMPSON (1979) provided a lucid exposition of KATZ' work, and analyzes several interesting examples. THOMPSON also described the finite-dimensional version of the isoperimetric theory that is developed in § 5, and analyzed examples of deadloading and hardloading in elasticity. The theory presented here is more general and more rigouros than that of KATZ and THOMPSON. More importantly, I believe that it is appreciably simpler, even in the finite-dimensional case.

The examples of §§ 3 and 4 are included for their pedagogical value. No originality is claimed for the results concerning these examples although the deriva-

tions presented here are new. In the chemical engineering literature JACKSON (1973) has obtained relations between stability properties and the shape of the solution branch in the η *vs.* ϕ bifurcation diagram (*cf.* § 4).

It should be remarked that the results concerning stability in isoperimetric problems are generally accepted in the literature concerning pendant liquid drops. See WENTE (1980) and references therein. The equivalent of the isoperimetric stability results have also been obtained in other special contexts, for example SHATAH & STRAUSS (1985).

The example of an elastic rod that is analyzed in § 6 has been a topic of investigation by many authors, the most comprehensive treatment being that of ANTMAN & ROSENFELD (1978, 1980). A phase-plane analysis similar to the one adopted here is contained in JAMES (1981), which paper concerns the case where W is nonconvex. The fact that the buckled branches can possess many folds even when W is convex, and especially the role played by constitutive hypothesis (6.4), is one contribution of this analysis, the other being the stability results under hard-loading.

It should be stressed that the only direct information furnished by the analysis of this paper concerns the eigenvalues of the purely static eigenvalue problem that arises when the Euler-Lagrange equations are linearized about an equilibrium. Accordingly, no rigorous stability result is immediately available. However, this static eigenvalue problem is important because in many physical examples it is the first step in a rigorous derivation of stability by Ljapunov's direct method. The expectations are that

(i) the properties of the eigenvalue problem determine the properties of the associated second variation,

(ii) the properties of the second variation determine whether the equilibrium is actually (in some sense) a local minimum of the energy, and

(iii) the energy is a Ljapunov functional for the underlying dynamical system.

It should be stressed that in addition to the purely static eigenvalue problem that is considered here, there is a second eigenvalue problem that bears on stability properties. This second eigenvalue problem is obtained from linearization of the underlying dynamic equations followed by separation of the time variable. In general this dynamic eigenvalue problem will be non-symmetric with complex spectrum. Nevertheless, in some physical examples it is possible to extract information about the location of the spectrum of the dynamic eigenvalue problem from the location of the spectrum of the static eigenvalue problem. Indeed, it would be highly disconcerting if the two eigenvalue problems gave different stability predictions. Further discussion of this point is deferred to a later work.

Acknowledgements. I am particularly indebted to Professors A. D. JEPSON, D. H. SATTINGER, J. F. TOLAND and H. F. WEINBERGER who gave extensive advice and criticism during the development of this work. I should also like to thank Professors R. ARIS, H. B. KELLER and R. LAUTERBACH who provided helpful comments and references.

This research was supported by a Senior Research Fellowship, Institute for Mathematics and its Applications, University of Minnesota.

References

ANTMAN, S. S., & G. ROSENFELD (1978), Global behavior of buckled states of nonlinearly elastic rods. SIAM Review **20**, p. 513. Corrigenda (1980) **22**, p. 186.

CHANDRASEKHAR, S. (1939), An Introduction to the Study of Stellar Structure. U. of Chicago Press.

CHOW, S. N., & R. LAUTERBACH (1985), A Bifurcation Theorem for Critical Points of Variational Problems. IMA Report # 179.

CRANDALL, M. C., & P. H. RABINOWITZ (1973), Bifurcation, Perturbation of Simple Eigenvalues and Linearized Stability. Archive for Rational Mechanics and Analysis **52**, pp. 160–192.

DAVIS, H. T. (1962), Introduction to Nonlinear Differential and Integral Equations, Dover, New York.

DECKER, D. W., & H. B. KELLER (1980), Multiple Limit Point Bifurcation. J. of Math. Anal. and Appl. **65**, pp. 417–430.

DECKER, D. W., & H. B. KELLER (1981), Path Following Near Bifurcation. Comm. Pure and Applied Math. **34**, p. 149.

ÉMDEN, R. (1907), Gaskugeln. Berlin and Leipzig.

ERICKSEN, J. L. (1975), Equilibrium of bars. J. of Elasticity **5**, pp. 191–201.

GEL'FAND, I. M. (1963), Some problems in the theory of quasilinear equations. Amer. Math. Soc. Transl. Series 2 Vol. **29**, pp. 295–381.

IOOSS, G., & D. D. JOSEPH (1980), Elementary Stability and Bifurcation Theory. Springer, New York.

JACKSON, R. (1973), A simple geometric condition for instability in catalyst pellets at unit Lewis number. Chemical Engineering Science **28**, pp. 1355–1358.

JAMES, R. D. (1981), The equilibrium and post-bucking behavior of an elastic curve governed by a non-convex energy. J. Elasticity **11**, pp. 239–269.

JOSEPH, D. D. (1979), Factorization Theorems and Repeated Branching of Solutions at a Simple Eigenvalue. Annals of the New York Academy of Sciences **316**, pp. 150–167.

JOSEPH, D. D., & T. S. LUNDGREN (1973), Quasilinear Dirichlet Problems Driven by Positive Sources. Arch. Rational Mech. Anal. **49**, pp. 241–269.

KATZ, J. (1978) (1979), On the number of unstable modes of an equilibrium I and II. Mon. Not. R. Astr. Soc. **183**, pp. 765–769, and **189**, pp. 817–822.

KELLER, H. B. (1977), Constructive Methods for Bifurcation and Nonlinear Eigenvalue Problems. Proc. 3rd Int. Symp. on Computing Method in Applied Science and Engineering.

MADDOCKS, J. H. (1984), Stability of nonlinearly elastic rods. Archive for Rational Mechanics and Analysis **85**, pp. 311–354.

MADDOCKS, J. H. (1985), Restricted quadratic forms and their application to bifurcation and stability in constrained variational principles. SIAM J. of Math. Anal. **16**, pp. 47–68.

MADDOCKS, J. H., & JEPSON, A. D. (1986), Exchange of stability in variational bifurcation problems. In preparation.

MEHTA, B. N., & R. ARIS (1971), A note on the form of the Émden-Fowler equation. J. Math. Anal. & Applications **36**, pp. 611–621.

SATTINGER, D. H. (1972), Stability of Solutions of Nonlinear Equations. J. Math. Anal. & Appl. **39**, pp. 1–12.

SHATAH, J., & W. STRAUSS (1985), Instability of nonlinear bound states. Comm. Math. Phys. **100**, pp. 173–190.

THOMPSON, J. M. T. (1979), Stability predictions through a succesion of folds. Phil. Trans. Roy. Soc. of London **192** A, p. 1386.

WEINBERGER, H. (1978), On the Stability of Bifurcating Solutions. Reprint from "Nonlinear Analysis" (dedicated to Erich Rothe), Academic Press.

WENTE, HENRY C. (1980), The Stability of the Axially Symmetric Pendent Drop. Pac J. of Math. **88**, pp. 421–469.

ZEIDLER, EBERHARD (1984), Nonlinear Functional Analysis and its Applications, Part III. Variational Methods and Optimization, Springer-Verlag, New York.

Department of Mathematics
University of Maryland
College Park

(Received February 8, 1987)